Applied Mathematics and Computation 379 (2020) 125249

Contents lists available at ScienceDirect

Applied Mathematics and Computation

journal homepage: www.elsevier.com/locate/amc

On the numerical stability of the exponentially fitted methods for first order IVPs☆

J.I. Montijano[a], L. Rández[a], M. Van Daele[b,*], M. Calvo[a]

[a] IUMA-Departamento Matemática Aplicada, Universidad de Zaragoza, 50009-Zaragoza, Spain
[b] Vakgroep Toegepaste Wiskunde, Informatica en Statistiek, Universiteit Gent, Krijgslaan 281-S9 B9000 Gent, Belgium

ARTICLE INFO

Article history:
Received 18 January 2020
Revised 26 March 2020
Accepted 29 March 2020
Available online 12 April 2020

MSC:
65L07

PACS:
02.60 Lj

Keywords:
Exponential fitting
Stability

ABSTRACT

In the numerical solution of Initial Value Problems (IVPs) for differential systems, exponential fitting (EF) techniques are introduced to improve the accuracy behaviour of classical methods when some information on the solutions is known in advance. Typically, these EF methods are evaluated by computing their accuracy for some test problems and it is usual to assume that the stability behaviour is similar to the underlying classical methods. The aim of this paper it to show that for some standard methods the stability behaviour of their exponentially fitted versions may change strongly. Furthermore, this stability depends on the choice of the fitting space, that must be carefully selected in order to assess the quality of the integrators for the IVPs under consideration. In particular, we will show that for the usual fitting space $\langle \exp(\omega x), \exp(-\omega x)\rangle$ with $\omega \in \mathbb{R}$ the size of the stability domain of the EF method can be much smaller than the one for the original method.

1. Introduction

Exponentially-Fitted (EF) methods (see [19] and references therein), developed after Gautschi's work [11] are designed to numerically integrate exactly problems whose solution belongs to a certain fitting space $\mathcal{S}$. This type of methods have been applied successfully to problems with oscillatory or exponential solutions.

In [27] for instance a mixed-type interpolation theory was used to construct EF linear multistep methods of Adams-type (for first order problems) and Milne- or Nyström-type (for second order problems) for which the fitting space $\mathcal{S}$ takes the form

$$\mathcal{S} = \langle \cos(\nu x),\ \sin(\nu x),\ 1,\ x,\ \ldots,\ x^{p-2}\rangle\,, \tag{1}$$

and whereby ν was locally chosen, based on the expression for the leading term of the local truncation error. For scalar first order problems $y' = f(x, y)$ for instance, this expression, when going from x_n to x_{n+1}, typically is of the form

$$C_{p+1}\, h^{p+1} \left(y^{(p+1)}(x_n) + \nu^2\, y^{(p-1)}(x_n)\right), \tag{2}$$

where C_{p+1} is some non-zero constant. The parameter ν^2 was then chosen such that the leading term vanishes, i.e. $\nu^2 = \nu_n^2$ whereby $y^{(p+1)}(x_n) + \nu_n^2\, y^{(p-1)}(x_n) = 0$. In this way, the coefficients of the method depend upon the product $(\nu h)^2$. Obvi-

☆ This work was supported by Ministerio de economia, industria y competitividad, project MTM2016-77735-C3-1-P

* Corresponding author.
E-mail addresses: monti@unizar.es (J.I. Montijano), randez@unizar.es (L. Rández), marnix.vandaele@ugent.be (M. Van Daele), calvo@unizar.es (M. Calvo).

https://doi.org/10.1016/j.amc.2020.125249
0096-3003/

ously, this is no problem for positive values of ν_n^2. For negative values of ν_n^2, one can put $\nu^2 = -\omega^2 = \nu_n^2$ and then the method is able to solve problems in the space spanned by

$$\begin{aligned}\mathcal{S} &= \langle \cosh(\omega x),\ \sinh(\omega x),\ 1,\ x,\ \ldots,\ x^{p-2}\rangle \\ &= \langle \exp(\omega x),\ \exp(-\omega x),\ 1,\ x,\ \ldots,\ x^{p-2}\rangle\,.\end{aligned}$$

Some standard methods (linear multistep [1,4,13,21], Runge-Kutta [2,9,14,18,20], Runge-Kutta Nystrom [10,22], Obrechkoff [5,23,26], General linear methods [7], Hybrid methods [8], Quadrature formulae [3,12],...) of this type were developed for different types of problems (first, second and also higher order problems; initial value problems and boundary value problems; eigenvalues problems; integro-differential problems, quadrature problems, etc.) in the past years. A unified approach to deal with the exponential and the trigonometric cases was proposed by Ixaru [16].

EF methods have been applied successfully in the past to numerically solve second order problems with (almost) periodic solutions. A lot of research was done on the construction of P-stable methods (e.g. [4,17,23,28]) for such problems. For first order problems however, things were different. While a lot of attention in the work on EF methods for first order problems was devoted to the choice of ν/ω, in order to optimize the numerical results, almost no attention ([6], [14] and [29] are some exceptions) was paid to the linear stability analysis of the methods. Probably, it was assumed that an EF method inherits its linear stability properties from its underlying polynomial method. Indeed, for small values of the fitting parameter(s), the region of stability of a method is closely related to that of the underlying method. For larger values, this is no longer the case.

In this paper, the linear stability properties of EF methods are studied. We will show that the size of the stability region of methods with the usual choice of the fitting space $\langle \exp(\omega x), \exp(-\omega x)\rangle$, $\omega \in \mathbb{R}$ can be substantially reduced, especially for methods intended to solve non stiff problems. To illustrate this fact, we consider EF variants for different fitting spaces for some well-known methods for first order problems: the explicit Euler method, a 2-stage explicit Runge-Kutta method, the 2-step Adams-Bashforth method and the 2-step Adams-Moulton method. Even though we will consider only these four methods, the results in this paper also hold for other methods that we examined, but we do not include them here for brevity.

The rest of the paper is organized as follows. In Section 2 we set the fitting space we are going to consider. In Section 3, we study the dependence of the stability region on the fitting space for Runge-Kutta methods with one and two stages. In Section 4 we do the analysis for Adams-Bashforth and Adams-Moulton methods and finally in Section 5 we summarize some conclusions of this study.

2. (*a, b*)-EF methods for first order problems

For a fitting space $\mathcal{S}$ containing $\langle \exp(\omega x), \exp(\theta x)\rangle$, we will assume that θ, ω can be real or complex conjugate. In the special case that $\theta = \omega \in \mathbb{R}$, we fit to a space $\mathcal{S}$ that contains $\langle \exp(\omega x), x\exp(\omega x)\rangle$ and if ω and θ both tend to 0, the EF method reduces to the classical underlying method.

Whereas for a standard step by step method its coefficients are constants, for EF methods they are allowed to depend on the products $a = \omega h$ and $b = \theta h$. Here, h is the (constant) step size, and a, b are the fitting parameters. In such a case, this method will be called (a, b)-EF method. In this paper a and b are either real, or else complex conjugate, in which case we denote them as $a = \alpha + i\beta$ and $b = \alpha - i\beta$ where $\alpha \in \mathbb{R}$ and $\beta \in \mathbb{R}^+$.

We want to emphasize that most of the EF-methods we discuss here are existing methods that have already been discussed or applied by various authors: (a, b)-EF methods with $a, b \in \mathbb{R}$ are typically considered in cases where the solution exhibits exponential behavior, while $(i\beta, -i\beta)$-EF methods are typically used for problems with a periodic, oscillatory behavior; $(\alpha + i\beta, \alpha - i\beta)$-EF methods on the other hand have already successfully applied to non-linear damped oscillator problems. The linear problem $y'' - 2\alpha y' + (\alpha^2 + \beta^2)y = 0$ is even exactly integrated by the $(\alpha + i\beta, \alpha - i\beta)$-EF method.

Previous research on EF methods (see e.g. [16,19]) has shown that when $a = -b \in \mathbb{R}$, the coefficients are continuous functions of a. However, when $a = i\beta = -b$, the coefficients become singular at certain values of β and therefore we should require that β is small enough. For many methods $\beta \in [0, \pi[$ is a common condition.

When a method is fitted to some fitting space $\mathcal{S}$, then the method is intended to be able to produce exact results for every problem for which the solution belongs to $\mathcal{S}$, whatever the size of h is. We should therefore be able to use step sizes which are quite large compared to those that can be used by classical methods and still attain machine accuracy. Thus in this discussion, we will focus on what happens when the absolute values of a and/or b (in the case of real fitting parameters) or α (complex fitting parameters) are not close to zero.

To analyse the linear stability properties of the methods, the scalar test equation

$$y' = \lambda y, \qquad y(0) = 1 \tag{3}$$

is used. Here $\lambda \in \mathbb{C}$ should be interpreted as a (possibly complex) eigenvalue of the (diagonalisable) matrix A in the differential system $y' = Ay$. In particular, the test equation (3) can be used to analyse the performance of a particular method on the problem $y'' + \omega_0^2 y = 0$ with the choice $\lambda = i\omega_0$.

Let $\mathcal{R}_{(a,b)}$ be the stability region of an (a, b)-EF method, i. e. the set of the points $h\lambda$ of the complex plane where the numerical solution of (3) is bounded. Given an (a, b)-EF method and the test problem (3) with a particular value of λ, the region $\mathcal{R}_{(a,b)}$ tells us which values of the step size h can be used to obtain a stable numerical solution. It also tells us, given

an $(a,\ b)$-EF method and a step size h, for which values of λ the test problem (3) can be solved in a stable way. So the stability region can tell us, given a method fitted to solve (3) for a particular value of λ exactly, whether a nearby problem can also be integrated adequately.

Let c be either $a=\theta\, h$ or $b=\omega\, h$ and let $z=\lambda\, h$. By construction, the numerical solution obtained after one step with an (a,b)-EF method coincides with the exact solution when $z=c$. For one step methods this ensures that, if $c\in\mathbb{C}^-$, then $z=c$ is in the stability region $\mathcal{R}_{(a,b)}$ of the $(a,\ b)$-EF method. However, we have no information about the location (near the border of close to the center) of z in $\mathcal{R}_{(a,b)}$. For multistep methods, the situation is worse. Choosing $z=c$ only means that one of the roots of the characteristic equation takes the value $\exp(c)$. However, we have no knowledge about the behaviour of the other roots of the characteristic equation. If one of these roots has a modulus that exceeds one, then the method, although particularly built to numerically solve $y'=\lambda\, y$ up to machine accuracy, is not capable to solve this problem in a stable way! In the next section, we pay attention to one step methods, in section 4, we will consider multistep methods. As mentioned earlier, we mainly focus on $(a,\ b)$-EF variants of methods with a relatively small region of stability $\mathcal{R}$ and we will study the behaviour of $\mathcal{R}_{(a,b)}$ as a function of $(a,\ b)$.

3. One step methods

Applying a one step method to the test equation (3) leads to a relation of the form

$$y_{n+1}=R(a,\ b;\lambda\, h)\, y_n$$

and the method is stable for those values of $z=\lambda\, h$ for which $|R(a,\ b;\ z)|\le 1$.

The specific form of R depends upon the method used. For explicit s-stage Runge-Kutta methods, as we consider in this section, it is known that R is a polynomial in z of degree s at most. However, given the space $\mathcal{S}$ the method is fitted to, it is also possible to determine R as an interpolating function, without explicitly constructing the method.

3.1. Euler's explicit method

As a first example, we consider EF variants of Euler's explicit method. In order to be able to fit the method to a space $\mathcal{S}$ containing two exponentials, we start from the expression (see [24])

$$y_{n+1}=\gamma\, y_n+h\, b_1\, f(x_n,y_n)\,.$$

Suppose we fit this method to the space $\mathcal{S}=\langle\exp(\omega\, x),\ \exp(-\omega\, x)\rangle$, we obtain (see [25])

$$y_{n+1}=\cosh(\omega\, h)\, y_n+h\,\frac{\sinh(\omega\, h)}{\omega\, h}\, f(x_n,\ y_n)\,.$$

It should be noted that this method is not consistent (as polynomial methods should be) since $\mathcal{S}$ does not contain the constant function. However, as ω tends to 0, the well-known explicit Euler method is found.

Applying this method to test problem (3) gives $y_{n+1}=R(\omega\, h,\ -\omega\, h,\ \lambda\, h)\, y_n$ where

$$R(a,\ -a;\ z)=\cosh(a)+z\,\frac{\sinh(a)}{a}\,.$$

One easily verifies that the interpolation conditions $R(a,\ -a;\ \pm a)=\exp(\pm a)$ are fulfilled.

Let us suppose $a=\omega\, h\in\mathbb{R}^-$. It is straightforward to show that $\mathcal{R}_{(a,-a)}$ is a disk in the complex z plane centered at $\delta=-\gamma/b_1=-a/\tanh(a)$ and radius $\rho=1/|b_1|=a/\sinh(a)$ (in the limit for $a\to 0$, which corresponds to Euler's explicit method, a disk with radius $\rho=1$ and center $\delta=-1$ is obtained). It is easy to see that ρ and δ monotonically decrease as a decreases, with

$$\lim_{a\to-\infty}\rho=0\qquad\lim_{a\to-\infty}\delta=-\infty\,.$$

This is shown in the left part of Figure 1. In the right part the intersection $[\delta-\rho,\delta+\rho]$ of $\mathcal{R}_{(a,-a)}$ and the negative real axis is shown. Clearly, the line $z=a$ falls into this region, but for very negative values of a, the interval of stability becomes very small, and only in a neighbourhood of $z=a$, which makes the method unattractive. In particular the $(a,\ -a)$-EF method is not zero-stable (one can in fact show that $a\, b\ge 0$ is required to obtain zero-stability) and provides unbounded numerical solutions for (3) with $\lambda\in\mathbb{R}^-$ near to zero.

To illustrate these theoretical results, we consider the test problem (3) with $\lambda=-4$ in the interval [0,20]. We choose $h=1$, such that $z=-4$ is fixed. For $\omega=\lambda$ (i.e. $a=z$) machine accuracy can be obtained, but what happens when we make a slight mistake in the choice of ω? In Figure 2 the results are shown when $\omega=0.95\,\lambda$, $\omega=\lambda$ and $\omega=1.05\,\lambda$. Clearly, we have instability in the first and the last case. An error of 5% in the choice of ω is fatal. As it is often the case in real applications that ω has to be estimated, this means that in practice the step size has to be chosen small enough.

Clearly, the choice for an $(a,\ -a)$-EF method with $a\in\mathbb{R}$ has a negative impact on the size of $\mathcal{R}_{(a,-a)}$. Let us therefore look at another choice for the parameters: we now consider $(a,\ b)=(\alpha+i\,\beta,\ \alpha-i\,\beta)$. The method then becomes

$$y_{n+1}=\exp(\alpha)\left(\cos(\beta)-\alpha\,\frac{\sin(\beta)}{\beta}\right)y_n+h\,\exp(\alpha)\,\frac{\sin(\beta)}{\beta}\,f(x_n,\ y_n)\,.$$

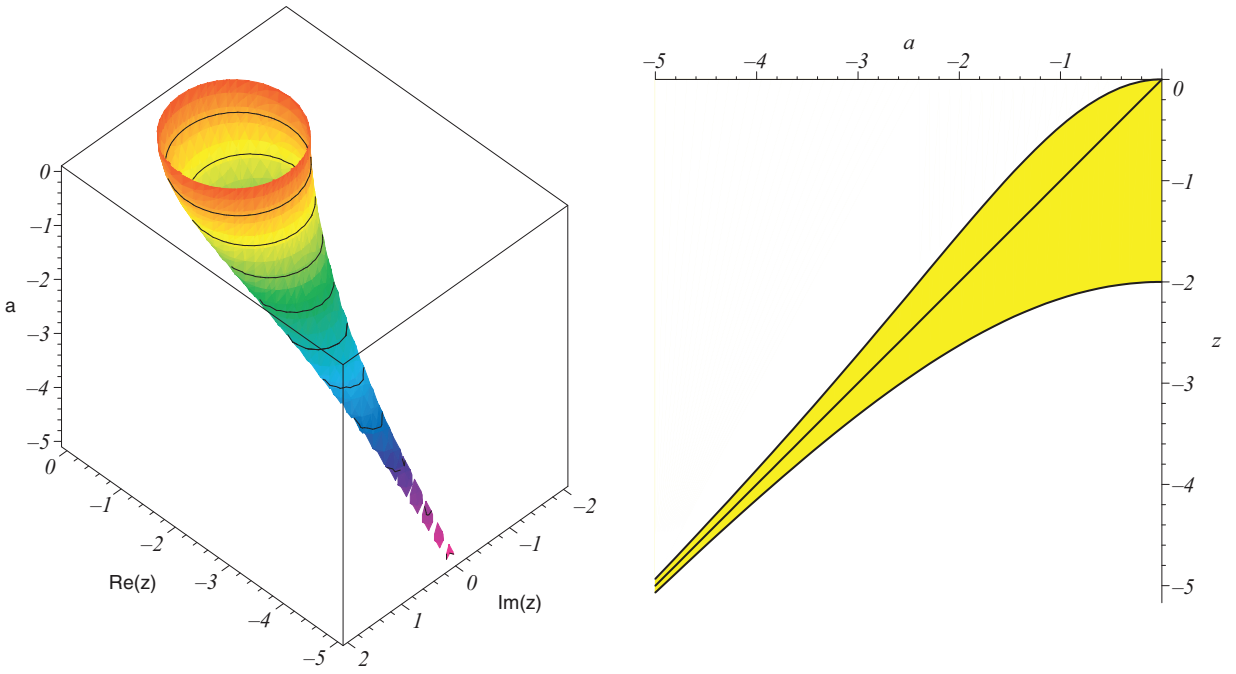

Fig. 1. Left: plot of the boundary of $\mathcal{R}_{(a,-a)}$ of the $(a,-a)$-EF Euler method as a function of a. Right: the intersection of $\mathcal{R}_{(a,-a)}$ and the negative real axis as a function of $a \in \mathbb{R}^-$.

and the stability function $R(a,b;z) = \tilde{R}(\alpha,\beta;z)$ is given by

$$\tilde{R}(\alpha,\beta,z) = \exp(\alpha)\left(\cos(\beta) + (z-\alpha)\,\frac{\sin(\beta)}{\beta}\right).$$

One easily verifies $\tilde{R}(\alpha,\beta,\alpha \pm i\,\beta) = \exp(\alpha \pm i\,\beta)$.

The stability region $\mathcal{R}_{(\alpha+i\beta,\alpha-i\beta)}$ is the interior of a disk centered at $\delta = \alpha - \beta/\tan(\beta)$ and with radius $\rho = \exp(-\alpha)\,\beta/\sin(\beta)$. In Figure 3, two contourplots are given to show the behavior of ρ (left) and δ (right) as a function of α and β. In the left part, the contours are shown where $\rho = 2^n$, $n = -1,\ldots,10$. For instance, at $\alpha = \beta = 0$ the radius is $2^0 = 1$. On the right, contours are drawn where $\delta = -5,\ldots,5$. One notices that at $\alpha = \beta = 0$ the disk $\mathcal{R}_{(\alpha+i\beta,\alpha-i\beta)}$ is centered at -1.

From Figure 3 and Figure 4, which particularly focusses on the cases $\alpha = 0$ and $\beta = 0$, we see that the radius ρ of $\mathcal{R}_{(\alpha+i\beta,\alpha-i\beta)}$ grows

- for fixed β, as α becomes more and more negative (at the same time the center δ moves to the left),
- for fixed α, as $\beta \in [0,\pi[$ becomes larger (at the same time the center δ moves to the right).

We remark that the last property enables us to conclude that all $(\alpha+i\beta,\alpha-i\beta)$-EF methods are zero-stable for $\alpha \le 0$. Indeed, the method is zero-stable for $\alpha \le 0$ and $\beta = 0$ since $0 \in [\delta-\rho,\delta+\rho] = [\alpha+1-\exp(-\alpha),\alpha-1+\exp(-\alpha)]$ and for increasing β the stability interval grows, while on the same time its center moves to the right.

When $\alpha = 0$ it is easy to show that for purely imaginary values of z stability is only obtained iff $|z| \le |\beta|$, i.e. β should be chosen large enough. We illustrate this with two examples whose results are depicted in Figure 5. In each case, we use $\lambda = i\,\omega_0 = i$, $h = \pi/10$ and the integration interval is $[0, 10\,\pi]$. First, we solve the problem with $\beta = \omega\,h$ where $\omega = 0.9\,\omega_0$ and it is found that the numerical solution grows, as was expected. Secondly, we use $\omega = 1.1\,\omega_0$ and the numerical solution decays.

To end this section on $(a,\ b)$-EF Euler methods, we can give following summary :

- when $b = -a \in \mathbb{R}$, the method looses its zero-stability property and $\mathcal{R}_{(a,-a)}$ shrinks as the parameter $|a|$ grows,
- when $a = \alpha + i\beta$ and $b = \alpha - i\beta$ are complex conjugate with $\beta < \pi$, zero stability is guaranteed for $\alpha \le 0$. The stability region grows as $|\alpha|$ and/or β grows.

We thus conclude that, for $(a,\ b)$-EF variants of Euler's explicit method, choosing the fitting parameters $(a,b) = (\alpha + i\,\beta, \alpha - i\,\beta)$ in general has a much better impact on the stability (especially along the negative real axis) than choosing $(a,b) = (a,-a)$.

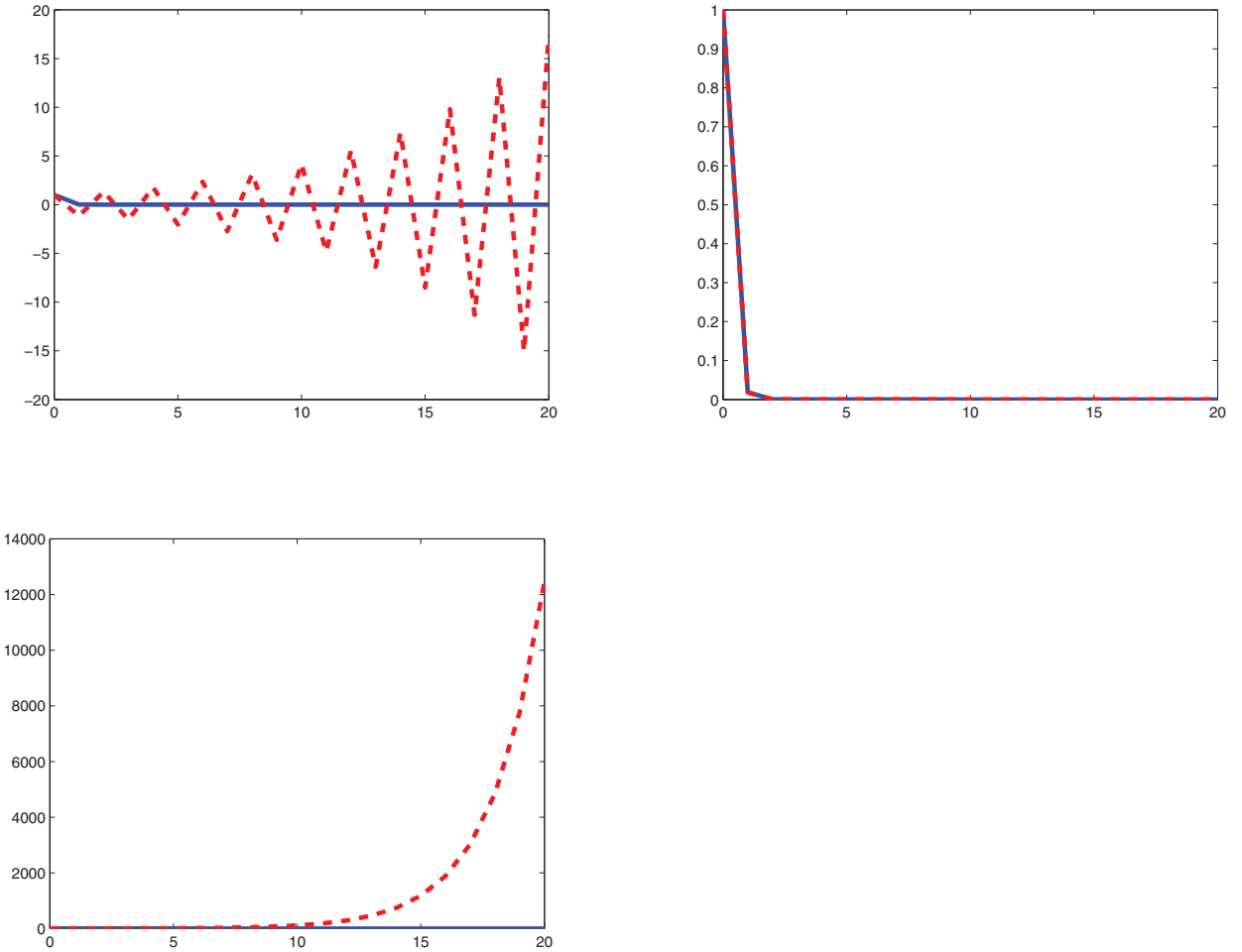

Fig. 2. The numerical (dashed line) and exact solution (solid line) when the $(a,-a)$-EF explicit Euler method is applied to $y'=-4y$ with step size $h=1$ in the interval [0,20] with (from left to right) $a=-3.8,\ -4,\ -4.2$.

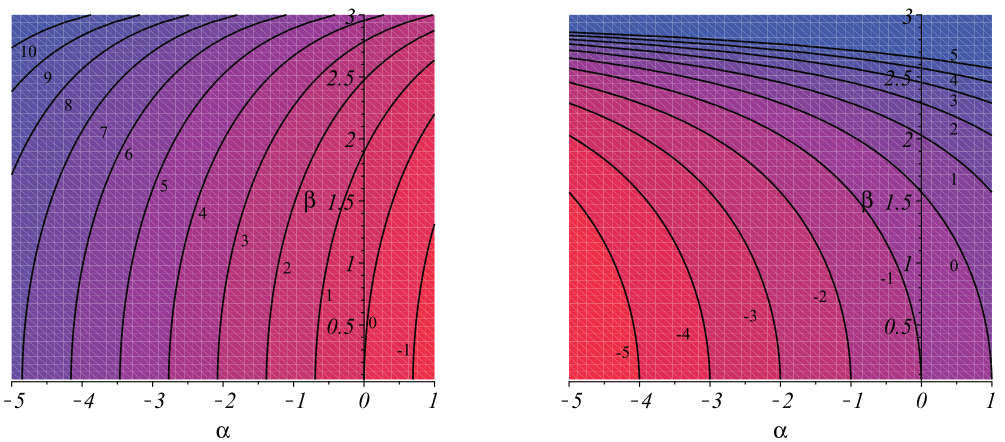

Fig. 3. Contourlines for $\log_2\rho$ whereby ρ is the radius (left) and for the center δ (right) of the disk representing $\mathcal{R}_{(\alpha+i\beta,\alpha-i\beta)}$ of the $(\alpha+i\beta,\alpha-i\beta)$-EF explicit Euler method.

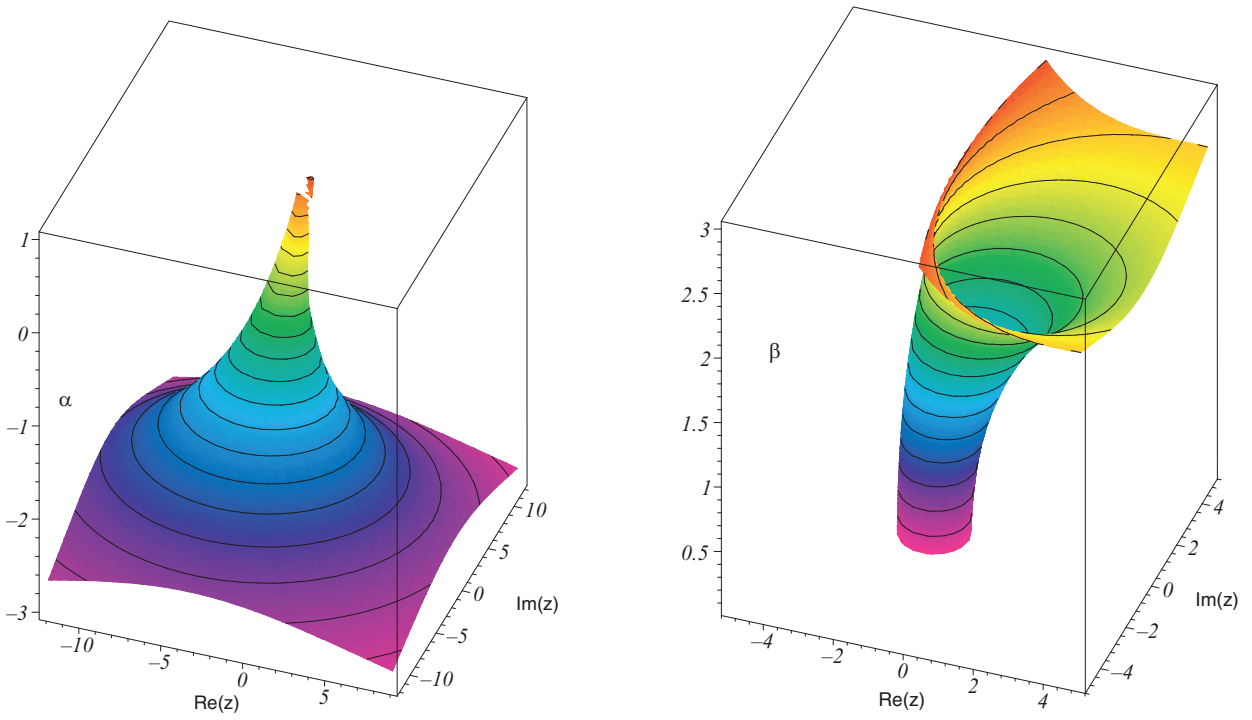

Fig. 4. Plots of the stability regions for $\beta = 0$ (left) and $\alpha = 0$ (right) of the $(\alpha + i\beta, \alpha - i\beta)$-EF explicit Euler method.

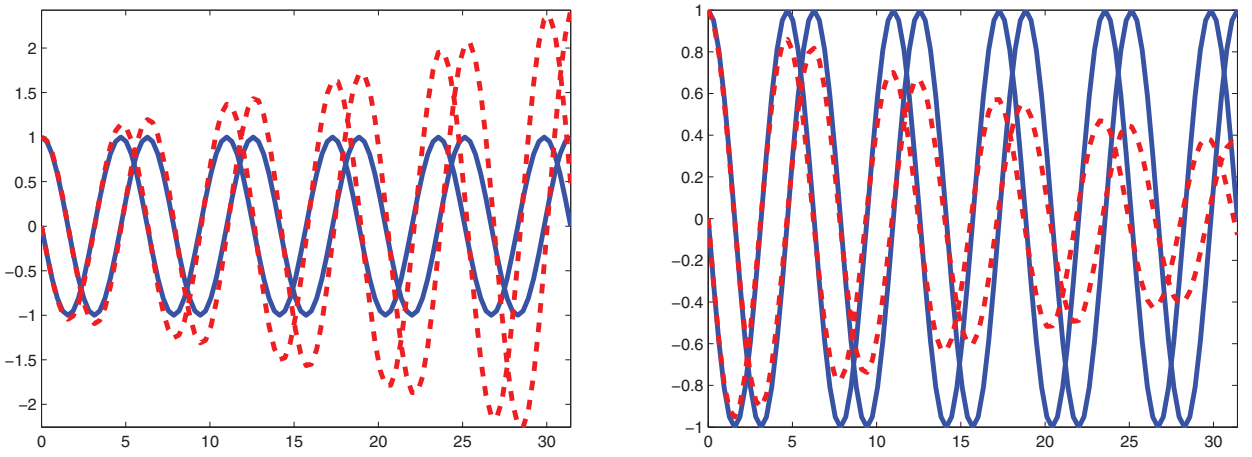

Fig. 5. The real and imaginary parts of the numerical (dashed line) and exact solution (solid line) when the $(i\beta, -i\beta)$-EF explicit Euler method is applied to (3) with $\lambda = i\omega_0 = i$ and step size $h = \pi/10$ in the interval $[0, 10\pi]$ with $\beta = 0.9\,\omega_0 h$ (left) and $\beta = 1.1\,\omega_0 h$ (right).

3.2. An explicit 2-stage RK method

We consider an EF Runge-Kutta method with modified tableau

$$\begin{array}{cccc} 0 & 0 & 0 & 0 \\ 1/2 & \gamma_2 & a_{21} & 0 \\ & \gamma & b_1 & b_2 \end{array}$$

where the second stage is fitted to $\langle \exp(\omega x), \exp(\theta x)\rangle$ and where the outer stage is fitted to $\langle 1, \exp(\omega x), \exp(\theta x)\rangle$.

For this method, we only consider the cases where $\theta = -\omega \in \mathbb{R}$ (i.e. $b = -a \in \mathbb{R}$) and $\theta = \omega \in \mathbb{R}$ ($b = a \in \mathbb{R}$). The coefficients for both cases are given below.

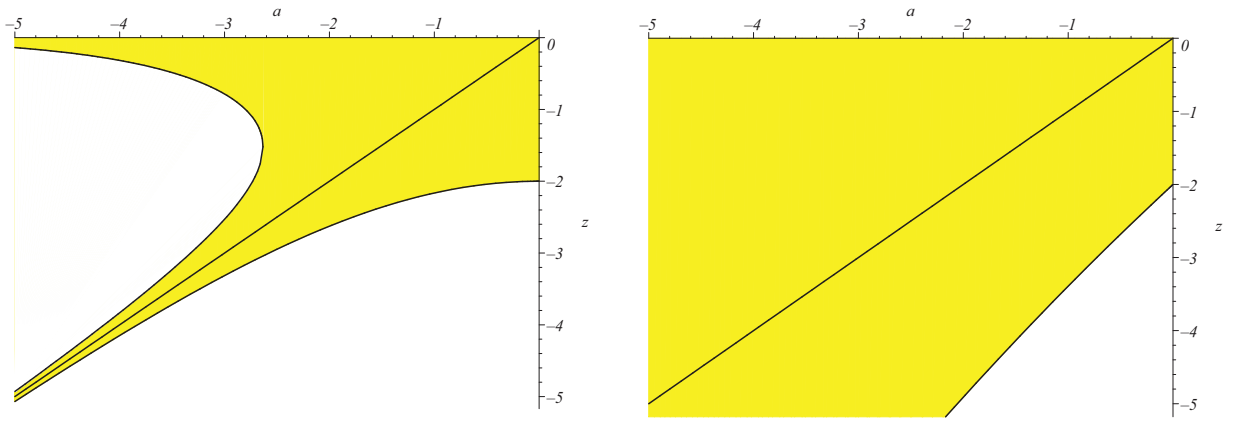

Fig. 6. Interval along the negative real axis for the $(a,-a)$-EF variant (left) and $(a,\,a)$-EF variant (right) of the 2-stage RK method.

- $\theta=-\omega$ $(a=\omega h=-b)$:

$$\begin{array}{ccc} 0 & 0 & 0 \\ 1/2 & \cosh(a/2) & \frac{\sinh(a)}{a} \\ & 1 & 0 \end{array} \qquad \begin{array}{c} 0 \\ 0 \\ \frac{\sinh(a/2)}{a/2} \end{array}$$

- $\theta=\omega$ $(a=\omega h=b)$: defining $u=\exp(a)$

$$\begin{array}{ccc} 0 & 0 & 0 \\ 1/2 & u\,(1-a) & u \\ & 1 & (u-1-a)/a^2 \end{array} \qquad \begin{array}{c} 0 \\ 0 \\ (u^{-1}-1+a)/a^2 \end{array}$$

In the case $a\to 0$ both methods reduce to

- $\theta=\omega=0$:

$$\begin{array}{ccc} 0 & 0 & 0 \\ 1/2 & 1 & 1 \\ & 1 & 0 \end{array} \qquad \begin{array}{c} 0 \\ 0 \\ 1 \end{array}$$

The classical 2-stage RK method has stability function $R(z)=1+z+z^2/2$, and the interval of stability is $[-2,\,0]$.

The stability function for both cases can be computed making use of the expressions for the coefficients. However, a much more elegant way (showing that the obtained result is independent of $c_2=1/2$) is to consider this as an interpolation problem and to start from a quadratic function $R(a,\,b;\,z)$ in z which passes trought the points (0,1), $(a,\,\exp(a))$, $(b,\exp(b))$:

$$R(a,b;z)=1+(\exp(b)-1)\,\frac{z\,(z-a)}{b\,(b-a)}+(\exp(a)-1)\,\frac{z\,(z-b)}{a\,(a-b)}\,.$$

Note that the point (0,1) is a consequence of adding the constant function to the fitting space of the outer stage (leading to $\gamma=1$).

One then obtains the following expressions :

- $R(a,-a;z)=1+\sinh(a)\,\dfrac{z}{a}+2\,\sinh^2(a/2)\left(\dfrac{z}{a}\right)^2$,
- $R(a,a;z)=1-\left(2-2\,e^a+ae^a\right)\dfrac{z}{a}+\left(ae^a+1-e^a\right)\left(\dfrac{z}{a}\right)^2$.

We now examine the behaviour of both expressions along the negative real axis as a function of $a\in\mathbb{R}^-$. Therefore, we put $z=r\,a$ and we consider what happens for $r\geq 0$. A detailed analysis shows that $R(a,\,a;\,r\,a)\geq 0$ for all values of $r\geq 0$, while $R(a,-a;r\,a)$ can become smaller than -1. Looking at the coefficient of r^2, we see that for $R(a,-a;r\,a)$ the coefficient can grow unboundedly, while in the $R(a,\,a;\,r\,a)$-case the coefficient is bounded by 1 for all $a\in\mathbb{R}^-$. As a consequence, the interval of stability for both methods is totally different, as can be seen in Figure 6. For both cases we have added the line $z=a,\ a<0$. In the $(a,-a)$ case this half line lies in the region where stable results are obtained, but when a becomes too negative, there is only a narrow region around $z=a$ for which there is stability, a similar situation as we encountered for the $(a,-a)$-EF explicit Euler method. Remark also that, as $|a|$ grows the coefficients of $(a,-a)$-EF RK methods become quite large, which also indicates that these methods are not suited for (too) large values of a. The left part of Figure 6 thus learns that the $(a,-a)$-EF method can only be used for small values of $|a|$, in which case the interval of stability has slightly grown compared to that of the classical method.

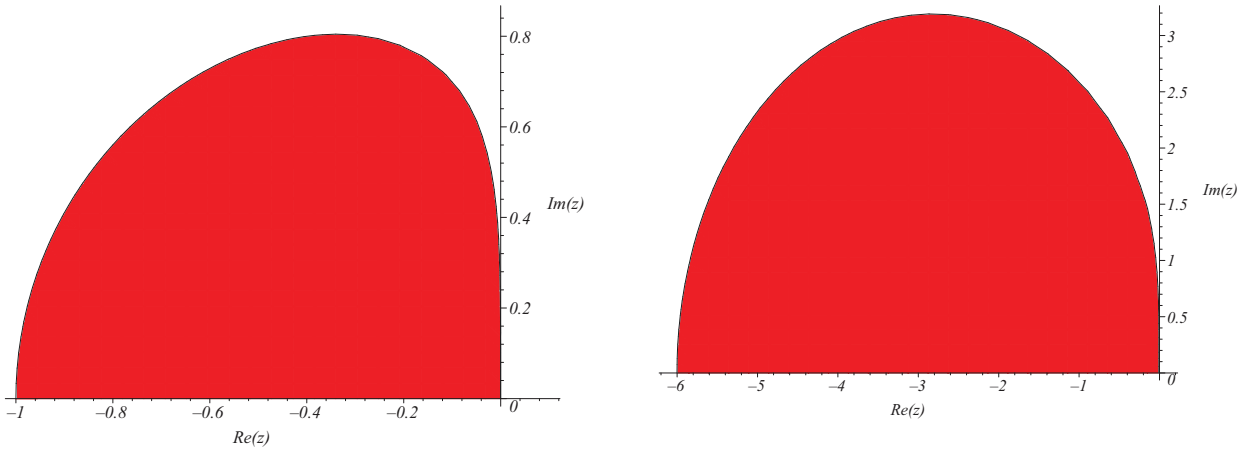

Fig. 7. Stability region of the classical two-step Adams-Bashforth method (left) and the classical two-step Adams-Moulton method (right).

For the (a, a)-case on the contrary, there is no problem. Already for small values of $|a|$ the interval of stabilty is quite larger than that of the classical method and even for large values the stability is guaranteed. Also, the coefficient of these (a, a)-EF methods remain small for a larger range of a-values.

Again, we can conclude that the choice $b = -a$ leads to poor stability properties along the negative real axis, while this is not the case for the choice $b = a$. In fact, one can show that when a and b are both real, much better stability properties are obtained when both a and b are negative and sufficiently close to each other, than when a and b have an opposite sign. This is however no surprise, having in mind that we can consider the construction of R as an interpolation problem: the behaviour of $R(a, b; z)$ for $z \in \mathbb{R}^-$ can be held under control much better when both interpolation conditions are imposed for $z < 0$.

4. Multistep methods

For multistep methods, we will see that requiring that an EF method can produce exact results for the test equation does no guarantee that the method can actually compute the solution in a stable way. The reason is that the numerical solution is a function of powers of all the roots of the characteristic equation. For a k-step method, there are k roots, but only one of them is more or less under control: the one, $r_1(z)$ say, that approximates the exponential function. Recall that for a polynomial method of order p, it is known (see e.g. [15]) that $r_1(z) - \exp(z) = \mathcal{O}(z^{p+1})$ as $z \to 0$.

Although the stability depends upon the roots of the stability function, we can also consider here an interpolation problem that gives some insight into the problem. Let $\rho(r)$ and $\sigma(r)$ be the first and second characteristic polynomials of an LMM. Then $\pi_S(r, z) := \rho(r) - z\sigma(r)$ is the stability polynomial of the method. Now consider the interpolating function

$$F(t) := \pi_S(\exp(t), t) = \rho(\exp(t)) - t\,\sigma(\exp(t))\,.$$

Suppose the LMM has fitting space $\mathcal{S}$. Then

$$(\langle \exp(\omega x),\, x\exp(\omega x),\, x^2\exp(\omega x),\, \ldots,\, x^q\exp(\omega x)\rangle \subset \mathcal{S} \Longleftrightarrow F(\omega h) = F'(\omega h) = \ldots = F^{(q)}(\omega h) = 0\,.$$

We remark that a polynomial method is of order p iff $F(h) = \mathcal{O}(h^{p+1})$ as $h \to 0$ (see e.g. [15]).

We consider two examples of LMM, an explicit one and an implicit one. Both methods have a relatively small region of stability and are well-suited to illustrate that the fitting space can have a substantial impact on the stability region of the EF-method.

4.1. The 2-step Adams-Bashforth method

The two-step Adams-Bashforth method, fitted to $\mathcal{S} = \langle 1, x, x^2\rangle$ is given by

$$y_{n+2} - y_{n+1} = h\,(b_1\,f(x_{n+1}, y_{n+1}) + b_0 f(x_n, y_n))$$

with $b_1 = \frac{3}{2}$ and $b_0 = -\frac{1}{2}$ and its stability region is shown in the left part of Figure 7.

The coefficients of the $(a, -a)$-EF variant are given by

$$b_0 = \frac{1 - \cosh(a)}{a\,\sinh(a)} \qquad b_1 = \frac{\cosh(2\,a) - \cosh(a)}{a\,\sinh(a)}\,.$$

One verifies that when $a = i\beta$ is purely imaginary, the coefficients become singular at $\beta = k\pi,\ k \in \mathbb{N}_0$. Therefore, we only consider $\beta \in [0, \pi[$.

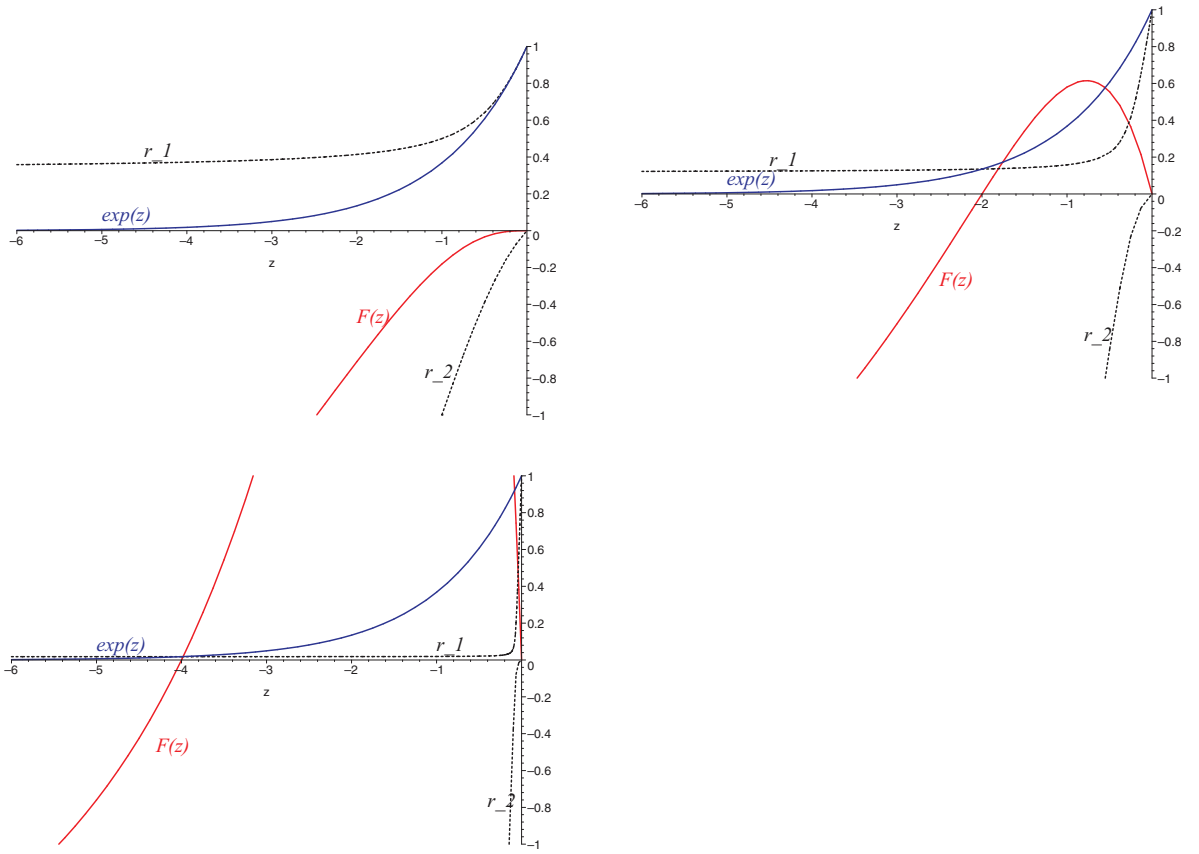

Fig. 8. Behavior of the roots r_1 and r_2 of the stability polynomial of the $(a, -a)$-EF 2 step Adams-Bashforth method for $a = 0$ (top), -2 (left) and -4 (right). Also $\exp(z)$ and the interpolation function $F(z)$ are shown.

The stability polynomial $\pi_S(r, \lambda h)$ of this method has the form

$$\pi_S(r, z) = (r - r_1)(r - r_2) = r^2 - (r_1 + r_2)\, r + r_1 r_2 = r^2 - (1 + b_1 z)\, r - z\, b_0$$

where the roots r_1 and r_2 not only depend upon $z = \lambda h$, but also on $a = \omega h$. By construction (see also the interpolation problem), we know that when $z = a$ (i.e. $\lambda = \omega$), one of these roots, say r_1, will be equal to $\exp(z) = \exp(a)$. The other root r_2 is the spurious root that might cause trouble. In this particular case, we find r_2 from $r_1 r_2 = -b_0 z$, and it turns out that

$$r_2 = \tanh(\lambda h/2)/\exp(\lambda h)\,.$$

The behaviour of the two roots, together with $\exp(z)$ and the interpolation function $F(z)$, is shown in Figure 8 for $a = 0,\ -2$ and -4. Clearly, as a becomes more and more negative, the z-value at which $r_2(z) = -1$ moves towards 0, resulting in a smaller region of stability $\mathcal{R}_{(a,-a)}$ than the original polynomial method.

Ideally, $|r_2| < 1$ for all $\lambda h \in \mathbb{C}^-$, but the left part of Figure 9, which displays the values of $z = \lambda h$ for which $|r_2| < 1$, shows that this is not the case. On the contrary, the result is very disappointing.

The method we constructed here is especially designed to solve the test problem (3) up to machine accuracy for any value of h, but this won't be the case for any value of λh. Indeed, when we look at the right part of Figure 9 where the stability regions (the interior part of the curves) of the $(a, -a)$-EF 2-step Adams-Bashforth methods are drawn, we see that the stability region shrinks as a becomes more and more negative. Once more, we see that the choice $(a, -a)$ has a negative influence on the stability properties.

Let's therefore consider the more general case $\mathcal{S} = \langle 1,\ \exp(\omega x),\ \exp(\theta x)\rangle$.

To start with, we consider the case where ω and θ are both real. The coefficients of the EF method are continuous functions that become however unbounded for large positive values of either $a = \omega h$ or $b = \theta h$. For large negative values of both a and b there is no problem.

We again consider what happens with the spurious root r_2 when the problem $y' = \lambda y$ is solved with one of the two parameters (say ω) put equal to λ. It then turns out that $r_1 = \exp(a)$ and

$$r_2 = \frac{a\,(\exp(b) - 1) - b\,(\exp(a) - 1)}{b\,(1 - \exp(a - b))}\,.$$

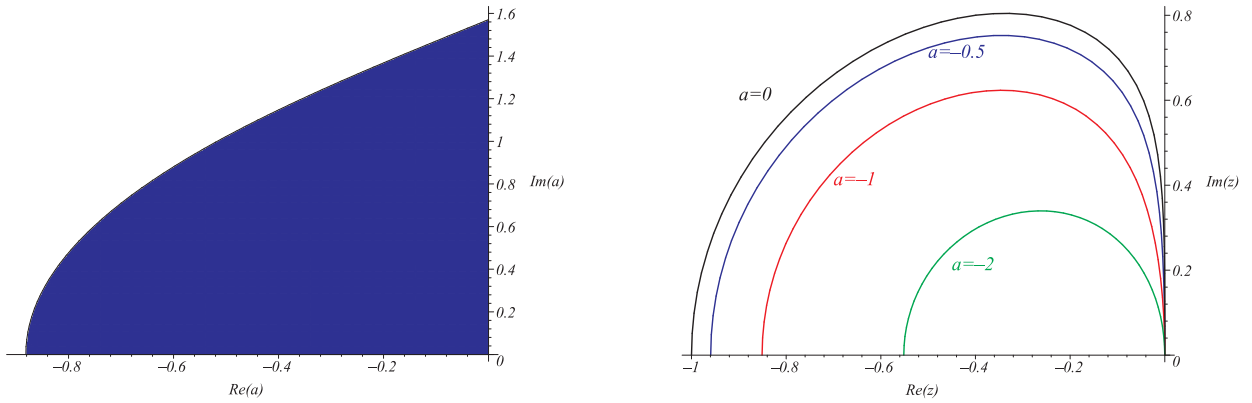

Fig. 9. Left : region of values $z = \lambda h$ for which the $(a, -a)$-EF two-step Adams-Bashforth method (fitted to $a = \lambda h$) can compute the solution of $y' = \lambda y$ in a stable way. Right : Stability region of the $(a, -a)$-EF 2-step Adams-Bashforth methods for $a = 0,\ -0.5,\ -1$ and -2.

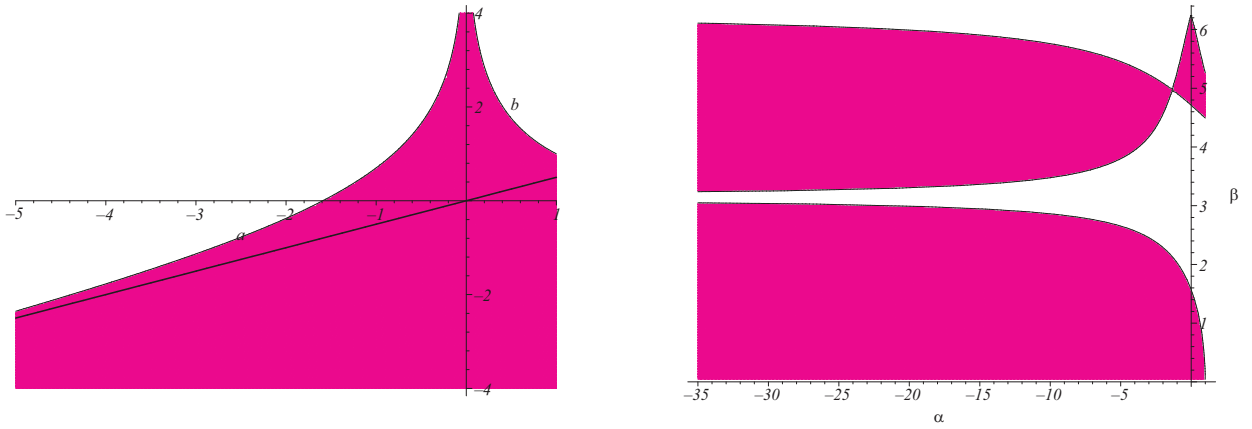

Fig. 10. Region of values $(a, b) \in \mathbb{R}^2$ (left) and $(a, b) = (\alpha + i\beta, \alpha - i\beta)$ (right) for which the (a, b)-EF two-step Adams-Bashforth method (fitted with $a = \omega h = \lambda h$) can compute the solution of $y' = \lambda y$ in a stable way.

In the left part of Figure 10, a contourplot of the region where $|r_2| \leq 1$ is shown. This picture shows that:

- when $b = -a$, i.e. $\theta = -\omega$, the modulus of the spurious root can become larger than 1 (it happens for example in the neighbourhood of $a = -b = -1$ which confirms Figure 9). In fact, the spurious root will cause problems for all combinations $(\omega, \theta) \in \mathbb{R}^- \times \mathbb{R}^+$ as h becomes too large,
- when a and b are both negative, it can be shown that the modulus of the spurious root remains bounded by 1 iff $b \leq a/2$ (this line is also displayed in the figure).

Some particular examples of stability regions are shown in Figure 11. We consider three cases ($b = -a$, $b = a/2$ and $b = a$) and for each of these cases we draw the boundary of the (bounded) stability region for $a = 0,\ -1,\ -3$ and -5. We note that the size of the stability region shrinks for $b = -a$ as a becomes more and more negative, while in the other two cases the size of the stability region grows. This can also be seen clearly in Figure 12, which in particular focusses on the intersection of the stability region with the real axis for the cases $b = -a$ and $b = a$, as was also done in Figure 6 for the 2-stage explicit RK methods.

In Figure 13, we show what happens with the roots r_1 and r_2 of the (a,a)-EF method when $a = -2$ and $a = -4$. Comparing with Figure 8, we notice that the behaviour of the spurious root r_2 is now completely different. In the $(a, -a)$-case we noticed that the point z_{-1} for which $r_2(z_{-1}) = -1$ grew from -1 towards 0 as a becomes more and more negative, thus resulting in a smaller and smaller stability region. In the (a, a)-case however, we now see that z_{-1} becomes more and more negative as a becomes more and more negative. As a consequence, the stability region for this (a, a)-EF method has grown, compared to the region of the underlying polynomial method.

Let us now also consider the case where $a = \alpha + i\beta$ and $b = \alpha - i\beta$ are complex conjugate with α negative and β positive. The coefficients now become unbounded as β approaches π. This means that we can only consider small values for β.

We again consider what happens with the spurious root r_2 when the problem $y' = \lambda y$ is solved with one of the two parameters (say ω) put equal to λ. In the right part of Figure 10, a contourplot of the region where $|r_2| \leq 1$ is shown.

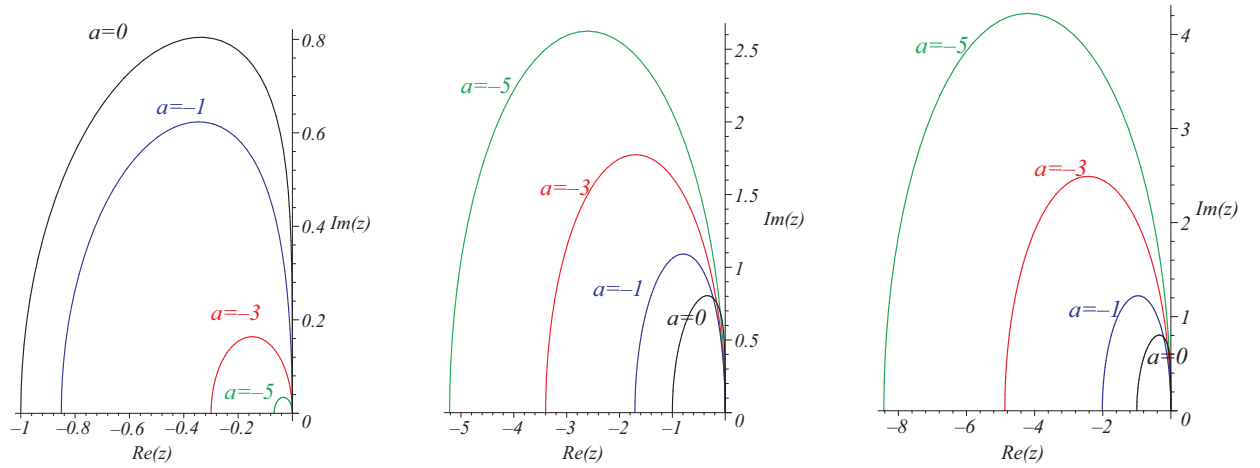

Fig. 11. Boundary of stability regions of the (a, b)-EF two-step Adams-Bashforth method with $b = -a$ (left), $b = a/2$ (middle) and $b = a$ (right) whereby $a = -5,\ -3,\ -1$ and 0.

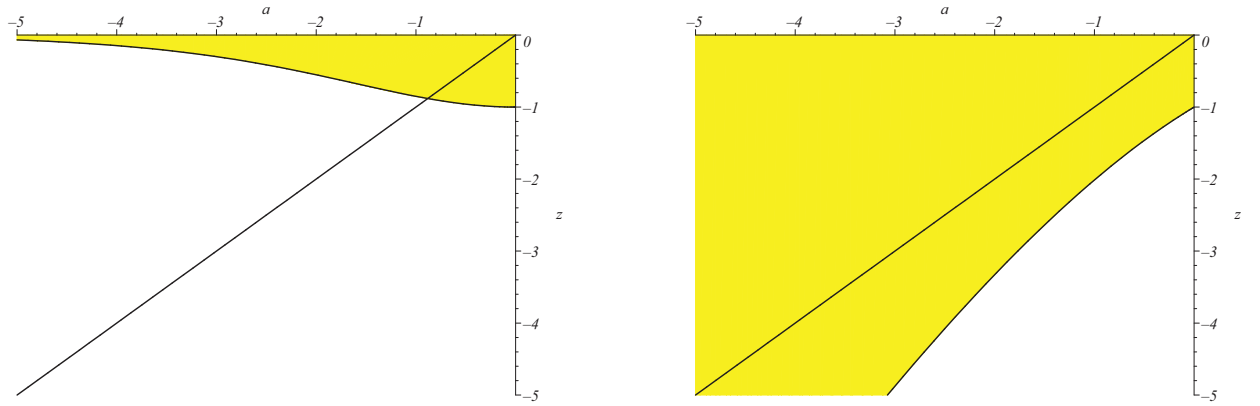

Fig. 12. Interval along the negative real axis for the $(a, -a)$-EF variant (left) and (a, a)-EF variant (right) of the 2-step Adams-Bashforth method.

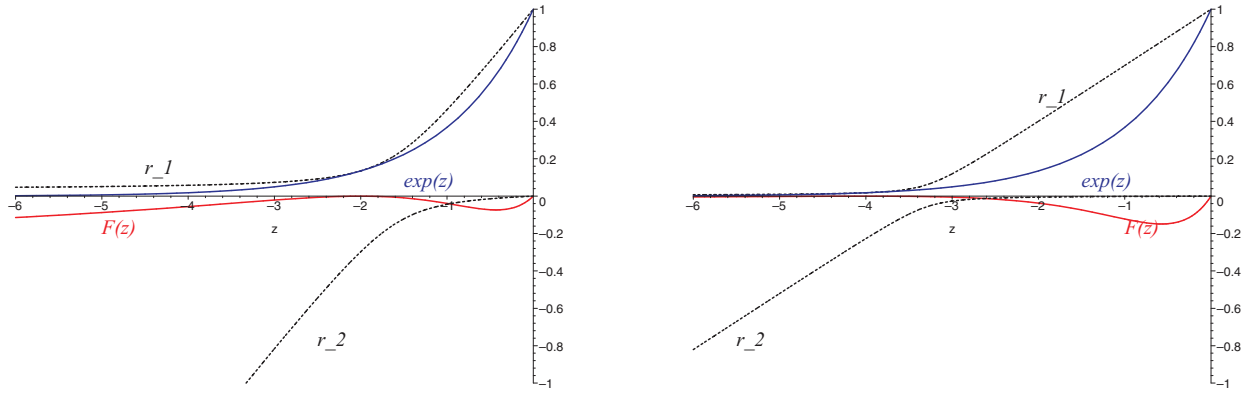

Fig. 13. Behavior of the roots r_1 and r_2 of the stability polynomial of the (a, a)-EF 2 step Adams-Bashforth method for $a = -2$ (left) and -4 (right). Also $\exp(z)$ and the interpolation function $F(z)$ are shown.

We notice that, along the line $\alpha = 0$, the method will only work for sufficiently small values of β (but this was already assumed), while along the axis $\beta = 0$ the modulus of the spurious root always remains bounded by 1, which means that the method will work well.

Also for the $(\alpha + i\beta, \alpha - i\beta)$-EF case we consider some examples, as shown in Figure 14. We consider three cases : $\alpha = 0$ (left), $\alpha = -1$ (middle) and $\alpha = -10$ (right). For each of these cases we draw the boundary of the stability region for $\beta = 0$, 1, 1.5 and 2. The stability region is the inner, bounded, part of the closed curve. We note that the stability area grows as

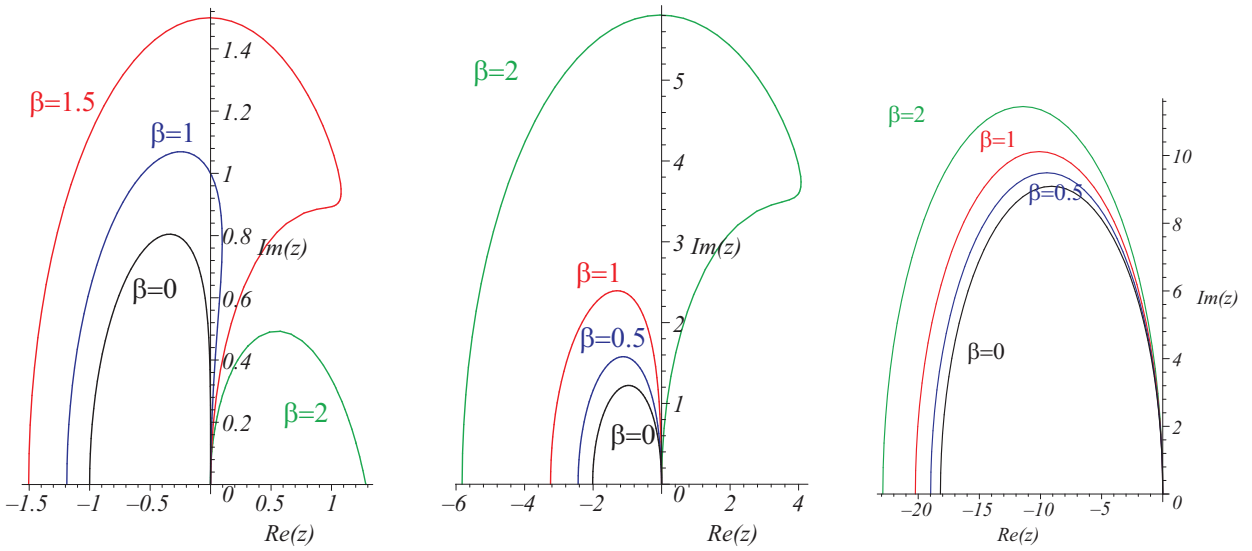

Fig. 14. Stability regions of the $(\alpha + i\beta, \alpha - i\beta)$-EF two-step Adams-Bashforth method. In the left part $\alpha = 0$, in the middle $\alpha = -1$ and in the right part $\alpha = -10$. For β the values 0, 1, 1.5 and 2 were taken.

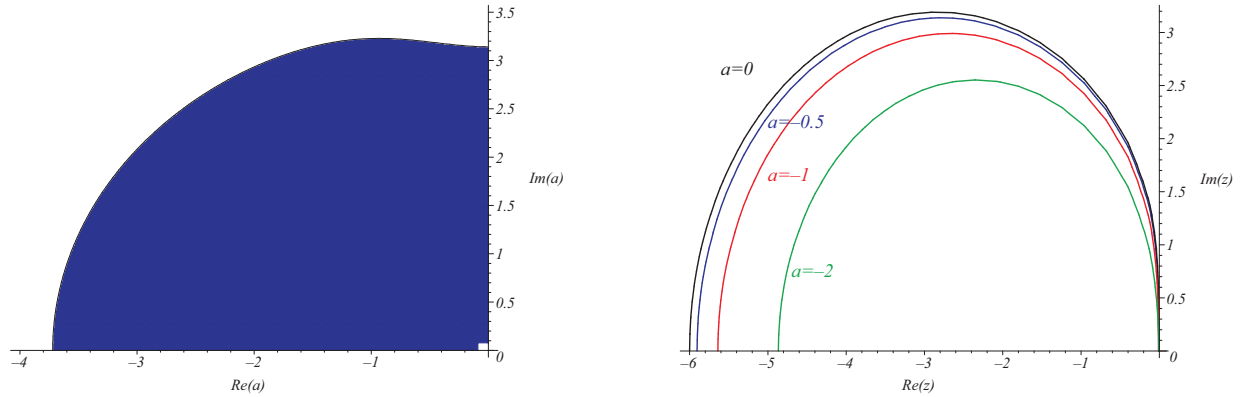

Fig. 15. Left : region of values $a = z = \lambda h$ for which the $(a, -a)$-EF two-step Adams-Moulton method can compute the solution of $y' = \lambda y$ in a stable way. Right : stability region of the $(a, -a)$-EF 2-step Adams-Bashforth method for $a = 0$, $a = -0.5$, $a = -1$ and $a = -2$.

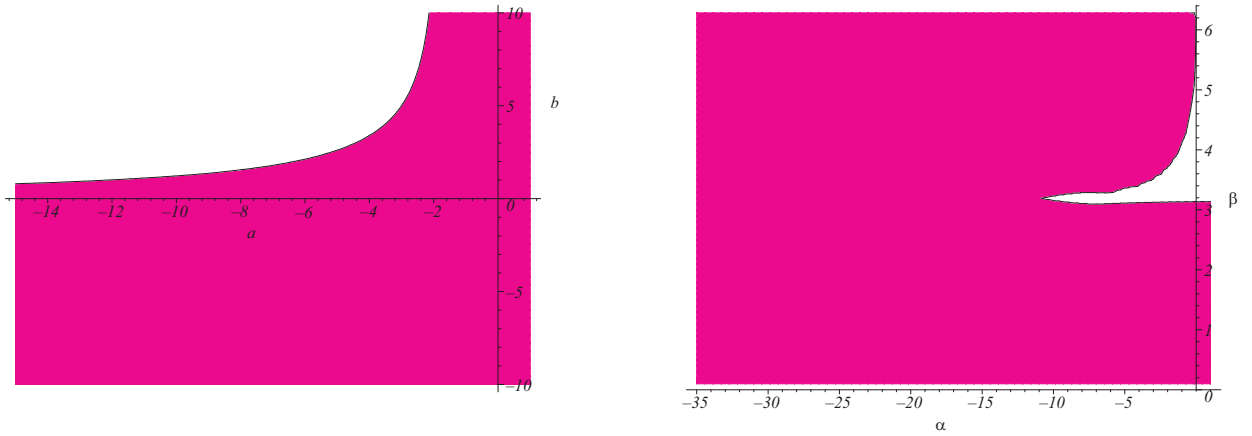

Fig. 16. Region of values $(a, b) \in \mathbb{R}^2$ (left) and $(a, b) = (\alpha + i\beta, \alpha - i\beta)$ (right) for which the (a, b)-EF two-step Adams-Moulton method (fitted with $a = \omega h = \lambda h$) can compute the solution of $y' = \lambda y$ in a stable way.

long as $\alpha + i\,\beta$ is in the stable area of the right part of Figure 10. In the case $\alpha = 0$, one can easily verify that $z = \beta\, i$ is on the border of the stability region, except for the case $\beta = 2$ (in which case the spurious root is dominant).

4.2. 2-step Adams-Moulton method

The classical form of this implicit method, fitted to $\mathcal{S} = \langle 1, x, x^2, x^3 \rangle$, is

$$y_{n+2} - y_{n+1} = h\,(b_2\, f(x_{n+2}, y_{n+2}) + b_1\, f(x_{n+1}, y_{n+1}) + b_0 f(x_n, y_n))$$

with $b_2 = \frac{5}{12}$, $b_1 = \frac{2}{3}$ and $b_0 = -\frac{1}{12}$ and its stability region is shown in the right part of Figure 7.

We have carried out a similar analysis for the EF 2-step Adams-Moulton method as we did for the EF 2-step Adams-Bashforth method. The conclusions we could draw for the Adams-Bashforth method also hold for the Adams-Moulton

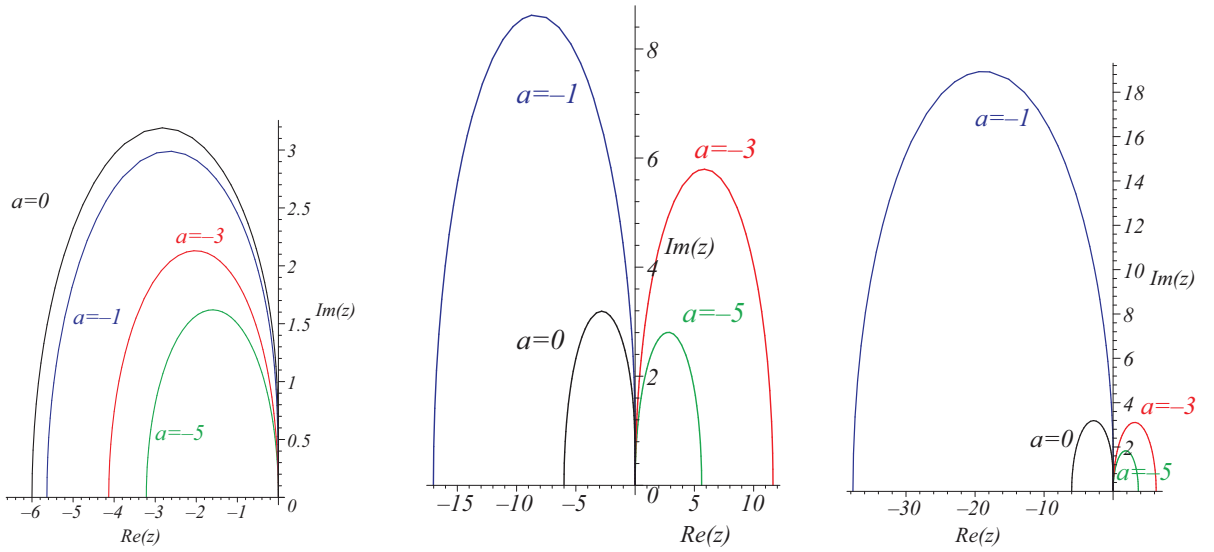

Fig. 17. Boundary of stability regions of the (a, b)-EF two-step Adams-Moulton method with $b = -a$ (left), $b = a/2$ (middle) and $b = a$ (right) whereby $a = 0$, -1, -3 and -5. For the curves in the left half plane, the stability region is bounded by the curve, for the curves in the right half plane, the stability region is the infinite outer part of the curve.

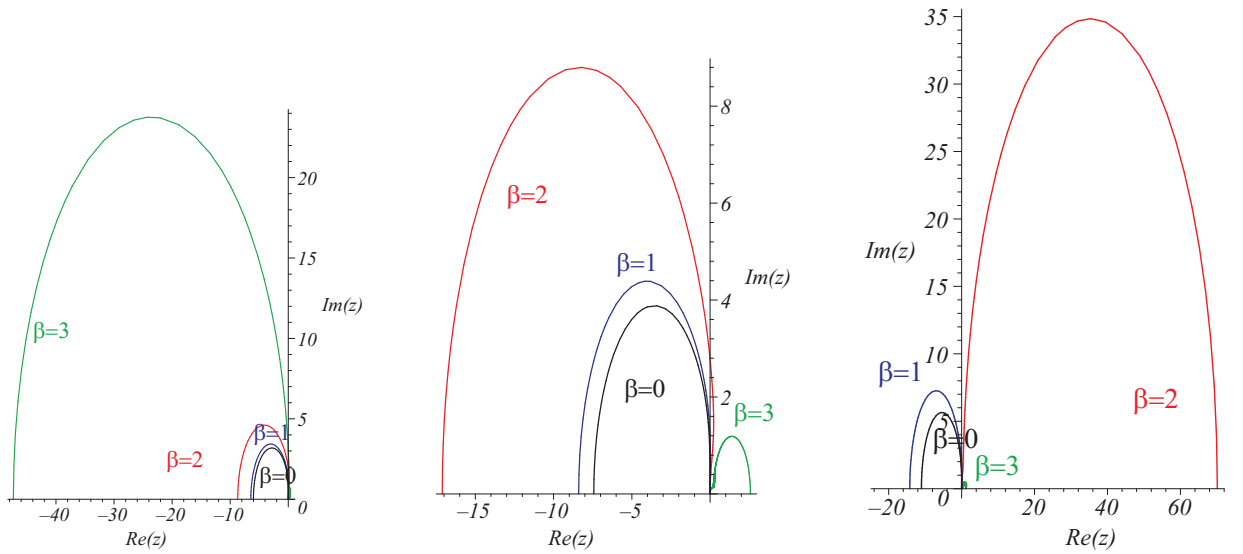

Fig. 18. Boundary of the stability regions of the $(\alpha + i\beta, \alpha - i\beta)$-EF two-step Adams-Moulton method. In the left part $\alpha = 0$, in the middle $\alpha = -0.2$ and in the right part $\alpha = -0.5$. For β the values 0, 1, 2 and 3 were taken. For the curves in the left half plane, the stability region is bounded by the curve, for the curves in the right half plane, the stability region is the infinite outer part of the curve.

method. Figure 15 for instance is the equivalent of Figure 9. Again, there is only a limited region for which the method can do what it is constructed for and we notice that as a becomes more and more negative the stability region shrinks.

Figure 16 is equivalent to Figure 10. The figure on the left again confirms that choosing (a, b) where $a < 0$ and $b > 0$ may be not such a good idea as far as stability is concerned, since this causes the stability region to shrink. Choosing both a and b negative leads to methods with enlarged stability region, as shown in Figure 17. We remark that there are combinations for which the stability region grows to an infinite region!

Also for the $(\alpha + i\beta, \alpha - i\beta)$-case we consider some examples, as shown in Figure 18. We consider three cases : $\alpha = 0$ (left), $\alpha = -0.2$ (middle) and $\alpha = -0.5$ (right). For each of these cases we draw the boundary of the stability region $\mathcal{R}_{(\alpha+i\beta,\alpha-i\beta)}$ for $\beta = 0,\ 1,\ 2$ and 3. We note that the stability area grows with decreasing α and with increasing β and also here the stability region can become infinitely large.

5. Conclusions

In this paper we have shown that the choice of the fitting space $\mathcal{S}$ greatly influences the size of the stability region and thus also the usefulness of the method, especially for methods that are EF variants of methods with a finite region of stability. We have shown that the traditional choice to fit to $\langle \exp(\omega x),\ \exp(-\omega x)\rangle$ with $\omega \in \mathbb{R}$ can be a very bad choice, as far as stability is concerned. This can be related to the fact that this linear space contains the solutions of the differential system $y'' - \omega^2 y = 0$, which represents an unstable dynamical system. In general, fitting to an increasing exponential function may cause the stability region to shrink compared to the stability region of the underlying polynomial method. A much better alternative, leading to increased stability, is to fit to two decreasing exponentials. In particular, when both functions coincide good results are found. To be able to cope with both the exponential and the trigonometric case, we therefore advocate the use of $\langle \exp(\omega x), \exp(\theta x)\rangle$, where ω and θ can both be real or complex conjugate, rather than of opposite sign.

Further, we have also shown that apart from the choice of the fitting space, also the choice of the parameters themselves is important. In real applications, it happens that their true values have to be estimated and for methods with poor stability properties this requires the use of small step sizes.

In conclusion, this paper has made it clear that the construction of useful EF-methods is not as straighforward as it seems. The research in this paper opens new questions about the stability of exponentially fitted methods. In future research we intend to study the effect that the fitting techniques have on the stability of implicit methods in the case of stiff problems. Also, the stability of EF methods applied to problems arising in the semidiscretization of hyperbolic problems, for which the region of stability around the imaginary axis is relevant, will be studied. In a near future we also plan to extend the research carried out to other class of numerical methods like exponentially fitted peer schemes.

References

[1] I. Alolyan, Z.A. Anastassi, T.E. Simos, A new family of symmetric linear four-step methods for the efficient integration of the schrödinger equation and related oscillatory problems, Appl. Math. Comput 218 (9) (2012) 5370–5382.
[2] M. Calvo, J.M. Franco, J.I. Montijano, L. Rández, Structure preservation of exponentially fitted runge-kutta methods, J. Comput. Appl. Math 218 (2) (2008) 421–434.
[3] A. IxaruCardone, L. Gr, B. Paternoster, Exponential fitting direct quadrature methods for volterra integral equations, Numer. Algorithms 55 (4) (2010) 467–480.
[4] J.P. Coleman, L.G. Ixaru, P-stability and exponential-fitting methods for $y'' = f(x, y)$, IMA J. Numer. Anal 16 (1996) 179–199.
[5] Y. Dai, Z. Wang, D. Wu, A four-step trigonometric fitted p-stable obrechkoff method for periodic initial-value problems, J. Comput. Appl. Math 187 (2006) 192–201.
[6] R. D'.Ambrosio, L. GrIxaru, B. Paternoster, Construction of the ef-based runge kutta methods revisited, Comput. Phys. Comm 182 (2011) 322–329.
[7] E. Esposito, B. Paternoster, R. D'Ambrosio, Exponentially fitted two-step runge-kutta methods: construction and parameter selection, Appl. Math. Comput 218 (14) (2012) 7468–7480.
[8] Y. Fang, X. Wu, A trigonometrically fitted explicit hybrid method for the numerical integration of orbital problems, Appl. Math. Comput 189 (2007) 178–185.
[9] J.M. Franco, An embedded pair of exponentially fitted explicit runge-kutta methods, J. Comput. Appl. Math 149 (2) (2002) 407–414.
[10] J.M. Franco, Exponentially fitted symplectic integrators of RKN type for solving oscillatory problems, Comput. Phys. Comm 177 (6) (2007) 479–492.
[11] W. Gautschi, Numerical integration of ordinary differential equations based on trigonometric polynomials, Numer. Math 3 (1961) 381–397.
[12] W. Gautschi, On the construction of gaussian quadrature rules from modified moments, Math. Comp 24 (1970) 245–260.
[13] D. Hollevoet, M.V. Daele, G.V. Berghe, The optimal exponentially-fitted numerov method for solving two-point boundary value problems, J. Comput. Appl. Math 230 (1) (2009) 260–269.
[14] D. Hollevoet, M.V. Daele, Exponentially-fitted methods and their stability functions, J. Comput. Appl. Math 236 (1) (2012) 4006–4015.
[15] E. Hairer, S.P. Nörsett, G. Wanner, Solving ordinary differential equations i (nonstiff problems), 2nd ed. (springer, berlin), 1993,
[16] L. Gr, G.V.B. Ixaru, Exponential Fitting, (Kluwer Academic Publishers, Dordrecht, 2004.
[17] L.G. Ixaru, B. Paternoster, A conditionally p-stable fourth-order exponential-fitting method for $y'' = f(x, y)$, J. Comput. Appl. Math. 106 (1) (1999) 87–98.
[18] A. París, L. Rández, New embedded explicit pairs of exponentially fitted runge-kutta methods, J. Comput. Appl. Math 234 (3) (2010) 767–776.
[19] B. Paternoster, Present state-of-the-art in exponential fitting, A contribution dedicated to Liviu Ixaru on his 70th birthday, Comput. Phys. Comm 183 (2012) 2499–2512.
[20] T.E. Simos, An exponentially-fitted runge-kutta method for the numerical integration of initial-value problems with periodic or oscillating solutions, Comput. Phys. Comm 115 (1) (1998) 1–8.
[21] T.E. Simos, Optimizing a class of linear multi-step methods for the approximate solution of the radial schrödinger equation and related problems with respect to phase-lag, Cent. Eur. J. Phys 9 (2011) 1518–1535.
[22] A. Tocino, J. Vigo-Aguiar, Symplectic conditions for exponential fitting runge-kutta-nyström methods, Math. Comput. Modelling 42 (2005) 7–8. 873–876
[23] M.V. Daele, G.V. Berghe, P-stable obrechkoff methods of arbitrary order for second-order differential equations, Numer. Algor. 44 (2007) 115–131.
[24] G.V. Berghe, H. De Meyer, M.V. Daele, T.V. Hecke, Exponentially-fitted explicit runge-kutta methods, Comput. Phys. Comm 123 (1999) 7–15.

[25] G.V. Berghe, Exponential fitting: General approach and applications for ODE-solvers, in: S. kalla, m. chawla (eds.), proceedings of the international conference of mathematics and its applications, kuwait university, ICMA, kuwait, 75–91, 2004,
[26] G.V. Berghe, M.V. Daele, Exponentially-fitted obrechkoff methods for second-order differential equations, Appl. Numer. Math 59 (2009) 3–4. 815–829
[27] J. Vanthournout, G.V. Berghe, H. De Meyer, Families of backward differentiation methods based on a new type of mixed interpolation, Comput. Math. Appl 20 (1990) 19–30. 1990
[28] J. Vigo-Aguiar, T.E. Simos, A family of p-stable eighth algebraic order methods with exponential fitting facilities, J. Math. Chem 29 (3) (2001) 177–189.
[29] J. Vigo-Aguiar, J. Martín-Vaquero, R. Criado, On the stability of exponential fitting BDF algorithms, J. Comput. Appl. Math 175 (2005) 183–194.